PRAMANA
— journal of
physics

Vol. 86, No. 4
April 2016
pp. 819–836

Cluster decay of $^{112-122}$Ba isotopes from ground state and as an excited compound system

K P SANTHOSH*, P V SUBHA and B PRIYANKA

School of Pure and Applied Physics, Kannur University, Swami Anandatheertha Campus, Payyanur 670 327, India

*Corresponding author. E-mail: drkpsanthosh@gmail.com

MS received 28 March 2014; revised 20 February 2015; accepted 11 March 2015

DOI: 10.1007/s12043-015-1084-7; ***e*Publication:** 23 September 2015

Abstract. The decay properties of various even–even isotopes of barium in the range $112 \leq A \leq 122$ is studied by modifying the Coulomb and proximity potential model for both the ground and excited state decays, using recent mass tables. Most of the values predicted for ground state decays are within the experimental limit for measurements ($T_{1/2} < 10^{30}$ s). The minimum $T_{1/2}$ value refers to doubly magic or nearly doubly magic Sn ($Z = 50$) as the daughter nuclei. A comparison of $\log_{10}(T_{1/2})$ value reveals that the exotic cluster decay process slows down due to the presence of excess neutrons in the parent nuclei. The half-lives are also computed using the Universal formula for cluster decay (UNIV) of Poenaru *et al* and the Universal decay law (UDL) of Qi *et al*, and are compared with CPPM values and found to be in good agreement. A comparison of half-life for ground and excited systems reveals that probability of decay increases with a rise in temperature or otherwise, inclusion of excitation energy decreases the $T_{1/2}$ values.

Keywords. Cluster decay; alpha decay.

PACS Nos 23.70.+j; 23.60.+e

1. Introduction

Cluster radioactivity is an exotic natural radioactivity in which a particle heavier than ^{4}He, but lighter than a fission fragment, is emitted. An important feature of this phenomenon is that decay products formed are in ground or the lowest excited state that contradicts the normal hot fission in which highly excited fragments are produced. This rare, cold phenomenon which forms an intermediate phenomenon between α decay and spontaneous fission was first theoretically predicted by Sandulescu *et al* [1] in 1980 based on the quantum mechanical fragmentation theory (QMFT). The fact that cluster emission is marked by several alpha emissions is the reason for the rare nature of this process. In 1984, Rose and Jones [2] experimentally observed this phenomenon in the radioactive decay of ^{223}Ra by emitting ^{14}C. Much efforts have been done on both experimental and theoretical fronts

for understanding the physics of cluster radioactivity. The next important step occurred in cluster studies is the observation of ^{24}Ne from ^{231}Pa by Tretyakova *et al* [3] in Dubna using solid-state nuclear track detectors (SSNTD). Intense experimental research led to the detection of about 20 cases of spontaneous emission from trans-lead nuclei with partial half-lives ranging from 10^{11} to 10^{28} s [4] emitting clusters ranging from ^{14}C to ^{34}Si. The common factor of all cluster radioactivity events is that the heavy-mass residue is found to be in the neighbourhood of the doubly-magic nucleus ^{208}Pb. This makes cluster radioactivity to be characterized as 'lead radioactivity' and indicates strong influence of shell effects on the nature of this phenomenon. On the basis of analytical superasymmetric fission model (ASAFM) [5] and preformed cluster model (PCM) [6], a second island of heavy-cluster radioactivity was predicted in the decays of some neutron-deficient rare-earth nuclei into ^{100}Sn ($Z = N = 50$) daughter or a neighbouring nucleus. Furthermore, another doubly closed ^{132}Sn ($Z = 50$, $N = 82$) daughter radioactivity was predicted by Kumar *et al* [6] for decays of some selective neutron-rich rare-earth nuclei. Experimentally, several unsuccessful attempts [7–10] have been made to measure the radioactivity of ^{100}Sn from the parent nucleus ^{116}Ba in ^{58}Ni + ^{58}Ni reaction. Spontaneous fission is also a competing decay channel in some heavy cluster emitters [11].

The theoretical models that are used to explain cluster radioactivity are classified as fission-like and alpha-like models. In fission-like model [12], the nucleus deforms continuously as it penetrates the nuclear barrier and reaches scission configuration after running down the Coulomb barrier. In alpha-like model [13–17], the cluster is assumed to be preformed in the parent nuclei before it penetrates the nuclear interacting barrier. Recently, Ni *et al* [18] proposed a unified formula of half-lives for α decay and cluster radioactivity to study the decay of even–even nuclei. Ren *et al* [19,20] analysed cluster radioactivity using microscopic density-dependent cluster model with the renormalized M3Y nucleon–nucleon interaction and reproduced cluster decay half-lives using a new formula.

In low-energy heavy-ion reactions, both the light ($A \approx 60$) and medium mass ($A \approx 110$) compound systems emit intermediate mass fragments (IMFs) with mass lighter than $A \approx 20$ and they arise as multiple clusters and are accompanied by multiple light particles ($Z \leq 2$). Light compound nuclei (CN) with mass number $A_{\rm CN} < 44$ that are formed in low-energy ($E/A <$ 15 MeV/nucleon) heavy-ion reactions are highly excited and carry large angular momenta. It was found that the decay process must depend on temperature- and angular momentum-dependent potential barriers. Cluster decay of $N = Z$, $A = 4n$ nucleus via α nuclei ($A_2 = 4n$, $Z_2 = N_2$) clusters was first pointed out in 1988 by Gupta and collaborators [21]. For very light nuclei with mass number $A \leq 80$ it was seen that the minima in potential energy surfaces lies always and only at α nuclei. Other clusters observed in the decay of radioactive nuclei also start appearing and become equally predominant for $N/Z \gg 1$ parents, as the N/Z ratio becomes larger than one.

As an extension of the phenomenon of exotic cluster radioactivity from various radioactive parents, the ^{12}C emission from $^{112-120}$Ba nuclei has been subjected to many theoretical [22–25] and experimental [26,27] investigations. A new phenomenon of emission of IMFs also referred to as 'clusters' or 'complex fragments' from excited compound system was observed in ^{58}Ni + ^{58}Ni $\rightarrow$ ^{116}Ba* reactions at both high ($E_{\rm cm} = 315$ MeV) [28,29] and medium ($E_{\rm cm} = 174$, 185.5, 187.5 and 197 MeV) energies [30,31]. The decay of Ba isotopes was first experimentally observed by Tretyakova *et al* [32] at Dubna and then by Guglielmetti *et al* [26] at GSI, Darmstadt. In all the experiments, ^{114}Ba

isotope ($Z = 56$) was produced using on-line mass separators by ^{58}Ni (^{58}Ni, $2n$) reaction. In Dubna experiments, polycarbonate track detectors and in GSI experiments phosphate glass detectors were used for searching carbon clusters. The experimental logarithm of half-life for ^{12}C decay from ^{112}Ba was found to be 3.75 s and that from ^{114}Ba was 4.23 s. These results however could not be reproduced in experiments [9] carried out in GSI in 1997, and hence the above half-life values are taken as the experimental lower limit. According to La Commara *et al* [31], this decay was assumed to be from the excited compound systems. As the half-life values fall within the experimental upper limits for measurements, ^{4}He, ^{8}Be, ^{12}C, ^{16}O and ^{20}Ne are predicted to be the possible decay modes of $^{112-120}$Ba.

In the present paper, we have studied the decay of various even–even Ba isotopes $^{112-122}$Ba by modifying the Coulomb and proximity potential model (CPPM) proposed by Santhosh *et al* [33] in 2000. We would like to mention that, using CPPM, the authors had performed the ground-state cluster decays of $^{116-124}$Ce isotopes [34] and $^{107-116}$Xe isotopes [35], which revealed the role of doubly magic ^{100}Sn daughter in cluster decay processes. The authors further modified CPPM by incorporating excitation energy and thus studied the cluster emission in superdeformed Sr isotopes formed in heavy-ion reaction [36]. The Coulomb and proximity potential model (CPPM) has been used extensively over the past decade for studying cluster/heavy particle decay [37–41], α-decay [42,43] and heavy-ion fusion [44]. In the present work, we have studied the decay of even–even $^{112-122}$Ba isotopes, by modifying the Coulomb and proximity potential model (CPPM), by incorporating the excitation energy and also by using the temperature-dependent radius, R_i and temperature-dependent surface diffuseness width, b. The present study looks into all aspects of α and cluster decay from these isotopes from both ground and excited states beginning with the identification of the most probable clusters from all isotopes. The decay properties have been studied and the results have been analysed to reveal the role of neutron and proton shell closure. The half-lives of these isotopes are computed and are compared with those values calculated using Universal formula for cluster decay (UNIV) of Poenaru *et al* [45] and Universal decay law (UDL) [46]. A plot of logarithmic half-life against fragment mass number is drawn for both the ground and the excited states decay.

The Coulomb and proximity potential model (CPPM) is presented in detail in §2, the results and discussion of the study are given in §3 and a conclusion of the entire work is given in §4.

2. The Coulomb and proximity potential model (CPPM)

The potential energy barrier, in the Coulomb and proximity potential model (CPPM), is taken as the sum of Coulomb potential, proximity potential and centrifugal potential for the touching configuration and for the separated fragments. The simple power-law interpolation done by Shi and Swiatecki [47] is used for the pre-scission (overlap) region. It is seen that the height of the potential barrier gets reduced when we include the proximity potential and it agrees closely with the experimental result. In our model in the penetrability calculations, contribution of both internal and external parts of the barrier is considered. In this model assault frequency ν is calculated for each parent–cluster

combination which is associated with vibration energy. But Shi and Swiatecki [48] got empirically unrealistic values of ν as 10^{22} for even-A parents and 10^{20} for odd-A parents.

The interacting barrier for a parent exhibiting exotic decay is given as

$$V = \frac{Z_1 Z_2 e^2}{r} + V_{\mathrm{P}}(z) + \frac{\hbar^2 \ell(\ell+1)}{2\mu r^2}, \quad \text{for } z > 0. \tag{1}$$

Here Z_1 and Z_2 are the atomic numbers of the daughter and the emitted cluster, r is the distance between fragment centres, z is the distance between the near surfaces of the fragments and ℓ represents the angular momentum. μ is the reduced mass given as $\mu = mA_1A_2/A$, where m is the nucleon mass and A, A_1 and A_2 are the mass numbers of the parent, daughter and the emitted cluster respectively. V_{P} is the proximity potential given by Blocki *et al* [49] as

$$V_{\mathrm{P}}(z) = 4\pi\gamma b\Big[\frac{C_1C_2}{C_1+C_2}\Big]\Phi\Big(\frac{z}{b}\Big). \tag{2}$$

Here, $r = z + C_1 + C_2$, where C_1 and C_2 are the Süsmann central radii of fragments. The nuclear surface tension coefficient is given as

$$\gamma = 0.9517[1 - 1.7826(N-Z)^2/A^2] \ \mathrm{MeV/fm^2}, \tag{3}$$

where N, Z and A are the neutron number, proton number and mass number of the parent, Φ is the universal proximity potential given as [50]

$$\Phi(\epsilon) = -4.41\mathrm{e}^{-\epsilon/0.7176}, \quad \text{for } \epsilon > 1.9475 \tag{4}$$

$$\Phi(\epsilon) = -1.7817 + 0.9270\epsilon + 0.0169\epsilon^2 - 0.05148\epsilon^3, \quad \text{for } 0 \le \epsilon \le 1.9475 \tag{5}$$

with $\epsilon = z/b$. The Süssmann central radii C_i of the fragments is related to the sharp radii R_i as $C_i = R_i - \big(b^2/R_i\big)$ and $b \approx 1$ fm is the width (diffuseness) of the nuclear surface. When the effect of temperature T is included, the surface width becomes

$$b(T) = 0.99(1 + 0.009T^2). \tag{6}$$

By the inclusion of nuclear temperature T, Süsmann central radii will be reformulated as

$$C_i = R_i(T) - \frac{0.99(1+0.009T^2)^2}{R_i(T)}. \tag{7}$$

For R_i, the semiempirical formula in terms of A_i is

$$R_i = 1.28A_i^{1/3} - 0.76 + 0.8A_i^{-1/3}. \tag{8}$$

For the excited compound system, the semiempirical formula can be written as

$$R_i(T) = (1.28A_i^{1/3} - 0.76 + 0.8A_i^{-1/3})(1 + 0.0007T^2). \tag{9}$$

The barrier penetrability P is given as

$$P = \exp\Big\{-\frac{2}{\hbar}\int_a^b \sqrt{2\mu(V-Q)}\mathrm{d}z\Big\}. \tag{10}$$

The inner and outer turning points a and b are defined as $V(a) = V(b) = Q$, where Q is the energy released. The half-life is given by

$$T_{1/2} = \left(\frac{\ln 2}{\lambda}\right) = \left(\frac{\ln 2}{\nu P}\right), \tag{11}$$

where λ is the decay constant and ν is the assualt frequency given as $\nu = (2E_{\rm v}/h)$. The empirical vibration energy $E_{\rm v}$ is given as [51]

$$E_{\rm v} = Q\left\{0.056 + 0.039\exp\left[\frac{(4 - A_2)}{2.5}\right]\right\}, \quad \text{for } A_2 \geq 4. \tag{12}$$

For the excited compound system, barrier penetrability P is given as

$$P = \exp\left\{-\frac{2}{\hbar}\int_a^b \sqrt{2\mu(V - Q_{\rm eff})}{\rm d}z\right\}, \tag{13}$$

where $Q_{\rm eff}$ is the effective Q value given as

$$Q_{\rm eff} = Q + E^*. \tag{14}$$

The temperature effects are included through a Boltzmann-like function

$$|\Psi|^2 = \sum_{v=0}^{\infty} |\Psi^v|^2 \exp\left(\frac{-E^v}{T}\right). \tag{15}$$

The excitation energy E^* related to the nuclear temperature T in MeV is given as

$$E^* = \frac{1}{9}AT^2 - T. \tag{16}$$

3. Results and discussions

The ground-state and excited state decay properties of various isotopes of Ba with $A =$ 112–122 emitting clusters with mass $A_2 =$ 4–56 have been studied within CPPM. The calculations are made by taking drifting potential as the sum of Coulomb and proximity potential for the touching configuration. The energy released in the cluster emission between the ground-state energy levels of the parent nuclei and the ground-state energy levels of the daughter nuclei is given as

$$Q = \Delta M - (\Delta M_1 + \Delta M_2) \tag{17}$$

and the possibility of cluster decay is related to its exotermicity, $Q > 0$. Here ΔM is the mass excess of the parent nuclei and ΔM_1 and ΔM_2 are the mass excesses of the daughter and the cluster nuclei respectively. The mass excess values for calculating Q values are taken from the recent mass tables of Wang *et al* [52] and for those isotopes whose mass excess values were unavailable in ref. [52], the corresponding values were taken from Koura–Tachibana–Uno–Yamada (KTUY) [53].

The concept of cold reaction valley is related to the minima in the so-called driving potential, which is defined as the difference between the interaction potential V and the Q value of the reaction. The driving potential of the compound nucleus is computed for all possible combinations of cluster and daughter for the touching configuration of fragments.

The most probable decay are represented as the minima in the driving potential which is due to the shell closure of one or both the fragments.

Figures 1–6 represent the cold valley plots of all the isotopes of Ba in the range $112 \leq A \leq 122$ in both ground and excited states. From figure 1, it can be seen that ^{8}Be, ^{12}C, ^{16}O, ^{20}Ne, ^{24}Mg, ^{28}Si, ^{32}S, ^{36}Ar, ^{40}Ca, ^{44}Ti, ^{48}Cr, ^{52}Fe and ^{56}Ni are the probable clusters. The minima in the driving potential are due to the shell closure of any of the fragments. In the case of ^{112}Ba, from the cold valley approach, the first deepest minima is seen at $^{12}\mathrm{C} + {}^{100}\mathrm{Sn}$ and it is due to the double magicity of ^{100}Sn ($Z = 50$, $N = 50$). The next minima is observed for the fragment combination $^{8}\mathrm{Be} + {}^{104}\mathrm{Te}$ and the near double magicity of ^{104}Te ($Z = 52$, $N = 52$) can be accounted for this minima. A minima can be observed for the splitting $^{56}\mathrm{Ni} + {}^{56}\mathrm{Ni}$ due to the presence of the doubly magic ^{56}Ni ($Z = 28$, $N = 28$). It is seen from the figures that the inclusion of temperature (excitation energy) does not change the position of the minima but it becomes deeper, i.e., the value of V–Q decreases with increase in temperature. This shows that the probability of cluster emission increases with increase in temperature in all the cases.

The $T_{1/2}$ values are calculated for the cluster decays of ^{112}Ba using CPPM at the ground state ($T = 0$ MeV) and the excited states ($T = 0.2$ MeV, 0.4 MeV, 0.6 MeV, 0.8 MeV and 1.0 MeV). The computed $\log_{10} T_{1/2}$ is plotted against fragment mass number in the case of ^{112}Ba isotopes for both ground and excited state decays which is shown in figure 7. It is seen that the inclusion of excitation energy decreases $T_{1/2}$ values and hence these nuclei become unstable against decay.

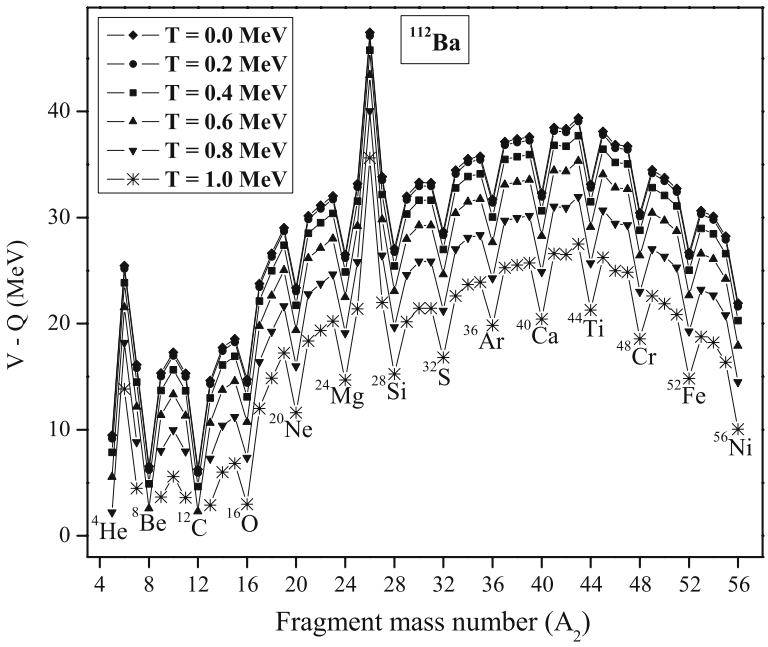

Figure 1. Cold valley plot for the binary fragmentation of ^{112}Ba at various temperatures.

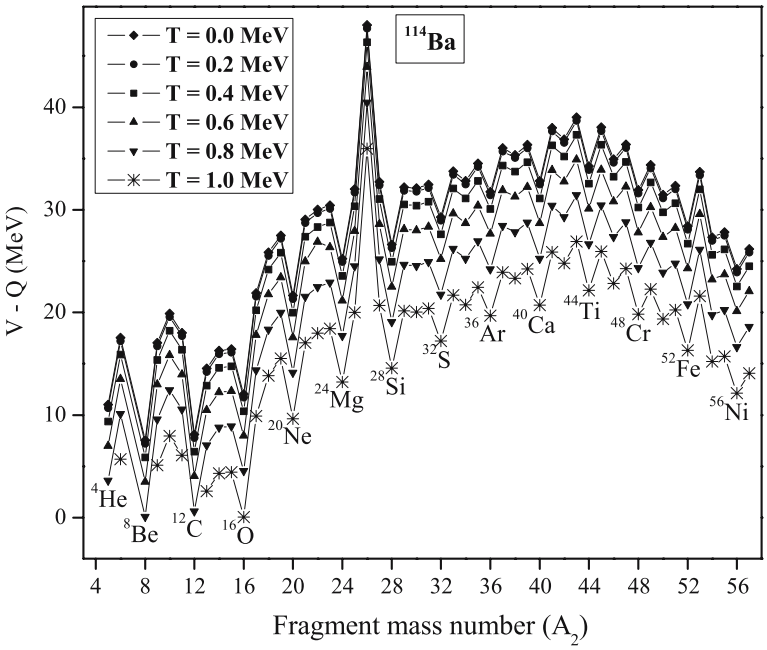

Figure 2. Cold valley plot for the binary fragmentation of ^{114}Ba at various temperatures.

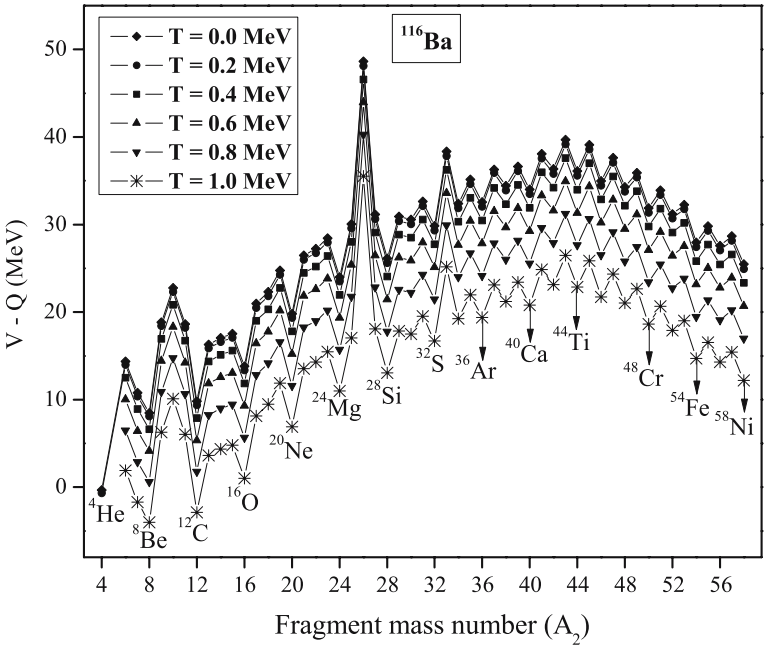

Figure 3. Cold valley plot for the binary fragmentation of ^{116}Ba at various temperatures.

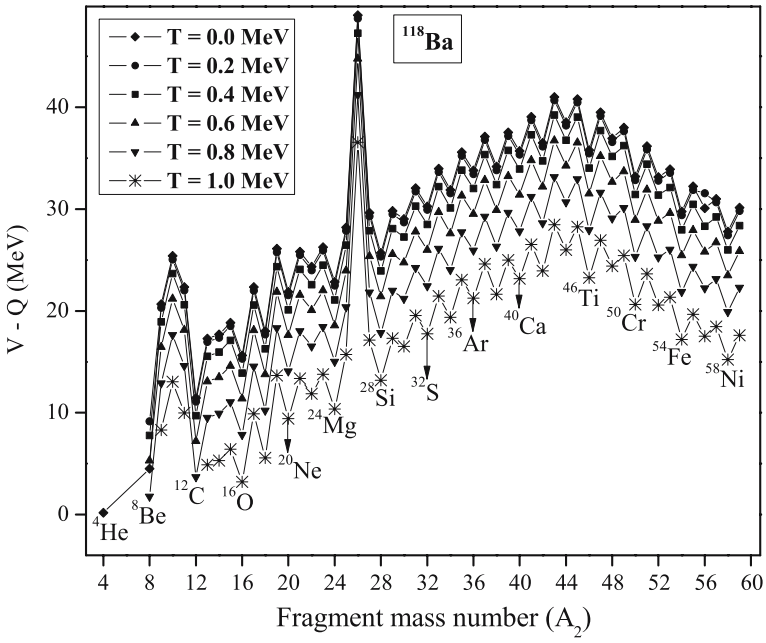

Figure 4. Cold valley plot for the binary fragmentation of ^{118}Ba at various temperatures.

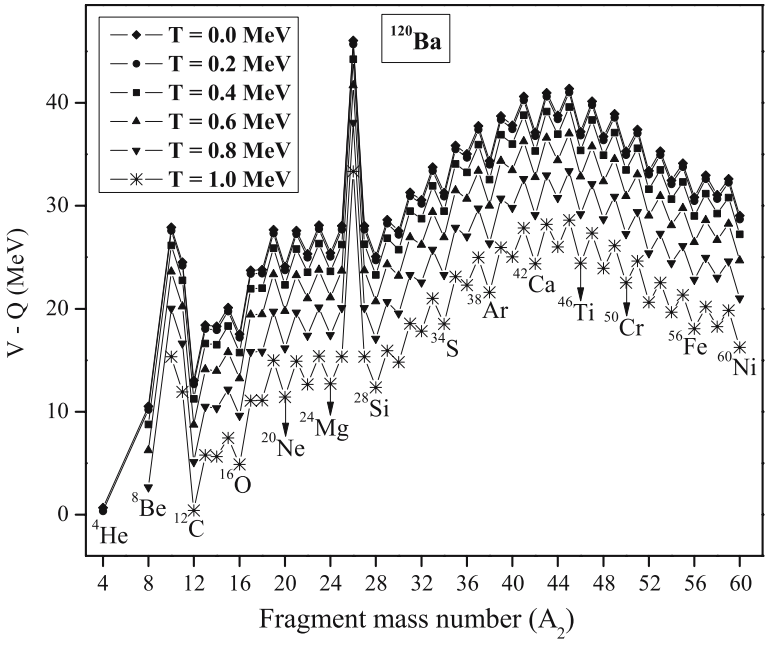

Figure 5. Cold valley plot for the binary fragmentation of ^{120}Ba at various temperatures.

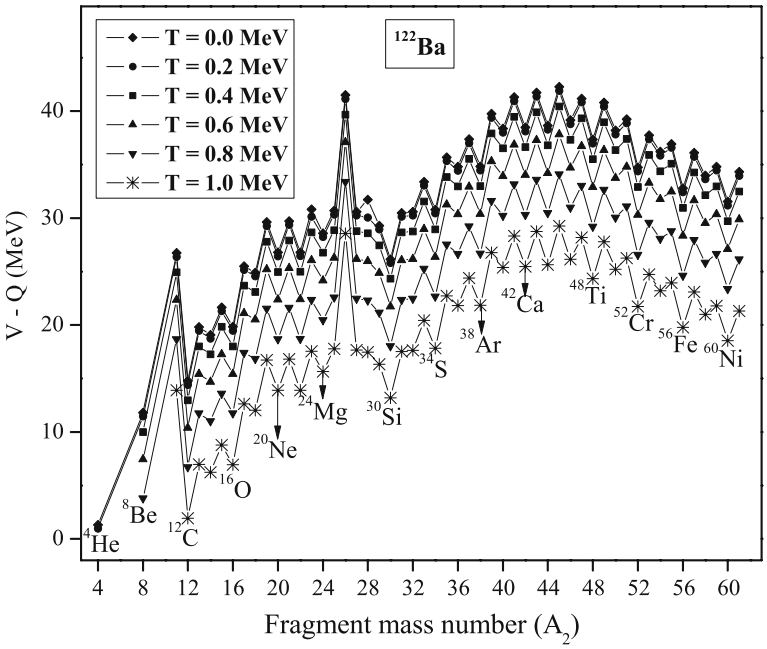

Figure 6. Cold valley plot for the binary fragmentation of ^{122}Ba at various temperatures.

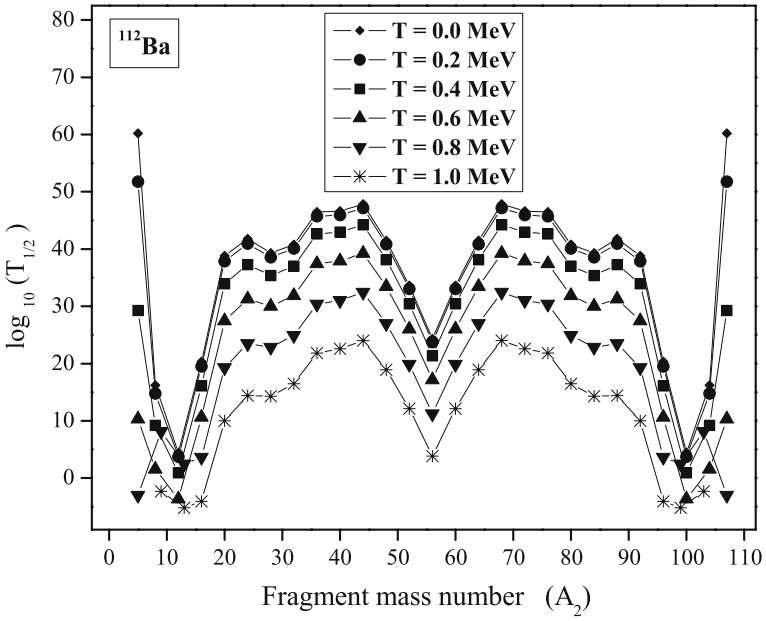

Figure 7. Variation of half-life with nuclear temperature for various clusters of ^{112}Ba.

The logarithmic half-life values are also computed using UNIV and UDL and are compared with those values calculated using CPPM. There are several relationships to compute cluster decay half-lives, whose parameters are obtained by the method of fitting the experimental data. Of these relationships, the universal curve (UNIV) [54–57] that is derived by extending fission theory to larger mass asymmetry is of great importance. The UNIV is based on quantum mechanical tunnelling process relationships [54,59] of disintegration constant λ, and is valid in both fission-like and α-like theories. The partial decay half-life T of the parent nucleus and disintegration constant λ is related as,

$$\lambda = \ln 2/T = \nu S P_s, \tag{18}$$

where T is the half-life and ν, S and P_s are the three model dependent quantities: S is the pre-formation probability of the cluster at the nuclear surface, ν is the assault frequency and P_s is the quantum penetrability of the external potential barrier. By using decimal logarithm

$$\log_{10} T(s) = -\log_{10} P - \log_{10} S + [\log_{10}(\ln 2) - \log_{10} \nu]. \tag{19}$$

The Universal formula is derived by assuming $\nu =$ a constant and S depends on the mass number of the emitted particle A_e [55,58]. A microscopic calculation of pre-formation probability [60] of clusters shows that it is indeed dependent only upon the size of the cluster. The corresponding numerical values [55] obtained by a fit with experimental data for α decay are: $S_\alpha = 0.0143153$, $\nu = 10^{22.01}\mathrm{s}^{-1}$. The additive constant for even–even nucleus can be taken as

$$c_{ee} = [-\log_{10} \nu + \log_{10}(\ln 2)] = -22.16917 \tag{20}$$

and the decimal logarithm of pre-formation factor is

$$\log_{10} S = -0.598(A_e - 1). \tag{21}$$

The penetrability of an external Coulomb barrier, having separation distance at the touching configuration $R_a = R_t = R_d + R_e$ as the first turning point and the second turning point defined by $e^2 Z_d Z_e / R_b = Q$, may be found analytically as

$$-\log_{10} P_s = 0.22873(\mu_A Z_e Z_d R_b)^{1/2} \times [\arccos\sqrt{r} - \sqrt{r(1-r)}]. \tag{22}$$

Here, $r = R_t/R_b$, $R_t = 1.2249(A_d^{1/3} + A_e^{1/3})$ and $R_b = 1.43998 Z_d Z_e / Q$. The liquid-drop model radius constant $r_0 = 1.2249$ fm and the mass tables [52,53] are used to calculate Q.

A new UDL for α-decay and cluster decay modes was introduced [46,61] starting from α-like (extension to the heavier cluster of α-decay theory) R-matrix theory. Moreover, in UDL, it is possible to represent logarithm of half-lives minus some quantity vs. one of the two parameters (χ' and ρ') that depend on atomic and mass numbers of the daughter and the emitted particle as well as the Q value on the same plot using a straight line. This law was introduced starting from the microscopic mechanism of the charged particle emission. The UDL relates the Q values of the outgoing particle with the half-life of monopole radioactive decay as well as the masses and charges of nuclei involved in the decay. In logarithmic form, UDL is written as

$$\log_{10}(T_{1/2}) = a Z_c Z_d \sqrt{\frac{A}{Q_c}} + b\sqrt{A Z_c Z_d (A_d^{1/3} + A_c^{1/3})} + c \tag{23}$$

$$= a\chi' + b\rho' + c, \tag{24}$$

where a, b and c are the coefficient sets of eq. (24) that are determined by fitting to experiments of both α and cluster decays [61] and are given by $a = 0.4314$, $b = -0.4087$ and $c = -25.7725$ and $A = A_d A_c/(A_d + A_c)$. The term $b\rho' + c$ include the effects that induce the clusterization in the mother nucleus. This relation holds for the monopole radioactive decays of all clusters and hence it is called the Universal decay law (UDL) [61].

In a similar manner, the cold valley plots have been drawn for the other Ba isotopes, i.e. $^{114-122}$Ba in both the ground and the excited states which are represented in figures 2–6. The shell closure effects of the fragments are analysed in all the cases. For all the isotopes, it is seen that the position of minima remains unaltered with rise in temperature but the driving potential decreases with increase in temperature which shows that the probability of cluster emission increases with increase in temperature. The computed half-lives are plotted against fragment mass numbers for all the above isotopes and are given in figures 8–12. The results show that $T_{1/2}$ values decrease with increase in temperature and hence the nuclei become unstable.

In tables 1 and 2, we have given the various decay characteristics such as the Q values, barrier penetrability, decay constant and half-lives for the emission of various clusters which lie in the minima of cold valley plot of all the even–even isotopes of Ba ($112 \leq A \leq 122$) in the ground state. Columns 1, 2 and 3 represent parent nuclei, emitted cluster and daughter nuclei respectively. Column 4 gives the Q values calculated using eq. (17) for $T = 0$ MeV. The penetrability and decay constant for the decays are calculated using

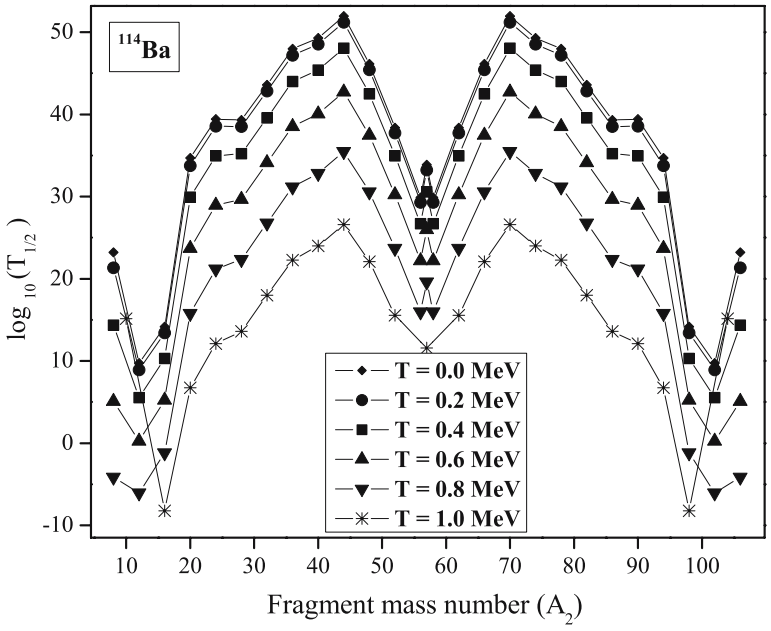

Figure 8. Variation of half-life with nuclear temperature for various clusters of ^{114}Ba.

Table 1. Computed logarithmic half-lives and other characteristics for the emission of clusters ^{4}He, ^{8}Be, ^{12}C, ^{16}O and ^{20}Ne from Ba isotopes and comparison of CPPM values with UNIV and UDL values.

Parent nuclei	Emitted cluster	Daughter nuclei	Q value (MeV)	Penetrability P	Decay constant	$\log_{10}(T_{1/2})$		
						CPPM	UNIV	UDL
^{112}Ba	^{4}He	^{108}Xe	4.065	3.529×10^{-21}	6.591×10^{-1}	0.022	−0.145	−1.408
^{114}Ba		^{110}Xe	3.535	2.093×10^{-24}	3.399×10^{-4}	3.309	2.967	1.836
^{116}Ba		^{112}Xe	2.901	2.213×10^{-29}	2.949×10^{-9}	8.371	7.784	6.819
^{118}Ba		^{114}Xe	2.311	1.122×10^{-35}	1.191×10^{-15}	14.765	14.119	13.294
^{120}Ba		^{116}Xe	1.732	6.009×10^{-45}	4.782×10^{-25}	24.161	23.384	22.607
^{122}Ba		^{118}Xe	1.045	7.615×10^{-65}	3.656×10^{-45}	44.278	43.081	42.584
^{112}Ba	^{8}Be	^{104}Te	8.598	1.554×10^{-37}	4.128×10^{-17}	16.225	15.951	16.041
^{114}Ba		^{106}Te	7.318	1.853×10^{-44}	4.189×10^{-24}	23.219	22.548	22.981
^{116}Ba		^{108}Te	6.140	1.125×10^{-52}	2.134×10^{-32}	31.512	30.473	31.225
^{118}Ba		^{110}Te	4.938	5.710×10^{-64}	8.710×10^{-44}	42.901	41.472	42.552
^{120}Ba		^{112}Te	3.736	2.185×10^{-80}	2.521×10^{-60}	59.439	57.607	59.018
^{122}Ba		^{114}Te	2.338	9.065×10^{-114}	6.548×10^{-94}	93.025	90.700	92.502
^{112}Ba	^{12}C	^{100}Sn	21.170	4.124×10^{-26}	2.432×10^{-5}	4.455	6.484	5.296
^{114}Ba		^{102}Sn	18.970	2.346×10^{-31}	1.239×10^{-10}	9.748	10.942	10.392
^{116}Ba		^{104}Sn	16.927	4.270×10^{-37}	2.013×10^{-16}	15.537	15.967	16.009
^{118}Ba		^{106}Sn	15.004	1.591×10^{-43}	6.650×10^{-23}	22.018	21.737	22.337
^{120}Ba		^{108}Sn	13.180	7.121×10^{-51}	2.614×10^{-30}	29.424	28.473	29.605
^{122}Ba		^{110}Sn	11.233	1.225×10^{-60}	3.833×10^{-40}	39.257	37.585	39.284
^{112}Ba	^{16}O	^{96}Cd	24.197	4.867×10^{-42}	3.208×10^{-21}	20.335	20.171	19.920
^{114}Ba		^{98}Cd	26.417	6.708×10^{-36}	4.826×10^{-15}	14.157	15.352	14.448
^{116}Ba		^{100}Cd	24.232	3.206×10^{-41}	2.116×10^{-20}	19.515	19.847	19.612
^{118}Ba		^{102}Cd	22.047	2.557×10^{-47}	1.535×10^{-26}	25.655	25.123	25.558
^{120}Ba		^{104}Cd	19.815	1.434×10^{-54}	7.742×10^{-34}	32.952	31.539	32.658
^{122}Ba		^{106}Cd	17.260	1.404×10^{-64}	6.598×10^{-44}	43.021	40.580	42.481
^{112}Ba	^{20}Ne	^{92}Pd	26.002	1.414×10^{-60}	9.971×10^{-40}	38.842	35.767	36.440
^{114}Ba		^{94}Pd	27.183	1.873×10^{-56}	1.381×10^{-35}	34.701	32.528	32.873
^{116}Ba		^{96}Pd	28.524	4.164×10^{-52}	3.221×10^{-31}	30.333	29.128	29.085
^{118}Ba		^{98}Pd	26.013	2.600×10^{-59}	1.834×10^{-38}	37.577	35.358	36.113
^{120}Ba		^{100}Pd	23.379	4.135×10^{-68}	2.621×10^{-47}	46.422	43.129	44.721
^{122}Ba		^{102}Pd	20.364	2.995×10^{-80}	1.654×10^{-59}	58.622	54.080	56.630

CPPM and is given in columns 5 and 6 respectively. The evaluated cluster decay half-lives using CPPM, UNIV and UDL are given in columns 7, 8, 9 respectively. The present upper limit for probable emission is $T_{1/2}$ values below 10^{30}s. The computed $T_{1/2}$ values are below this limit and hence probable for emission. It is also seen that the inclusion of excitation energy decreases $T_{1/2}$ values and hence these nuclei become unstable against decay. It is found that $T_{1/2}$ values computed using UNIV and UDL are in good agreement with those computed using CPPM.

Table 2. Computed logarithmic half-lives and other characteristics for the emission of clusters ^{24}Mg, ^{28}Si, ^{32}S, ^{36}Ar and ^{40}Ca from Ba isotopes and comparison of CPPM values with UNIV and UDL values.

Parent nuclei	Emitted cluster	Daughter nuclei	Q value (MeV)	Penetrability P	Decay constant	$\log_{10}(T_{1/2})$		
						CPPM	UNIV	UDL
^{112}Ba	^{24}Mg	^{88}Ru	32.224	1.291×10^{-63}	1.127×10^{-42}	41.789	38.186	38.044
^{114}Ba		^{90}Ru	32.858	2.884×10^{-61}	2.567×10^{-40}	39.431	36.557	36.251
^{116}Ba		^{92}Ru	33.535	7.106×10^{-59}	6.455×10^{-38}	37.031	34.876	34.386
^{118}Ba		^{94}Ru	34.168	1.110×10^{-56}	1.027×10^{-35}	34.829	33.340	32.674
^{120}Ba		^{96}Ru	31.123	4.974×10^{-65}	4.193×10^{-44}	43.218	40.374	40.714
^{122}Ba		^{98}Ru	27.550	1.391×10^{-76}	1.038×10^{-55}	54.825	50.366	51.883
^{112}Ba	^{28}Si	^{84}Mo	39.883	3.097×10^{-61}	3.345×10^{-40}	39.316	36.487	34.616
^{114}Ba		^{86}Mo	39.643	3.221×10^{-61}	3.459×10^{-40}	39.302	36.821	35.062
^{116}Ba		^{88}Mo	39.480	4.654×10^{-61}	4.977×10^{-40}	39.144	37.005	35.332
^{118}Ba		^{90}Mo	39.316	5.985×10^{-61}	6.372×10^{-40}	39.036	37.193	35.605
^{120}Ba		^{92}Mo	39.411	3.307×10^{-60}	3.530×10^{-39}	38.293	36.852	35.263
^{122}Ba		^{94}Mo	32.297	6.485×10^{-81}	5.673×10^{-60}	59.087	53.983	54.785
^{112}Ba	^{32}S	^{80}Zr	45.426	9.217×10^{-63}	1.134×10^{-41}	40.786	38.231	34.848
^{114}Ba		^{82}Zr	43.996	1.431×10^{-65}	1.706×10^{-44}	43.609	40.776	37.907
^{116}Ba		^{84}Zr	42.737	3.691×10^{-68}	4.272×10^{-47}	46.210	43.140	40.733
^{118}Ba		^{86}Zr	41.635	1.621×10^{-70}	1.828×10^{-49}	48.579	45.309	43.316
^{120}Ba		^{88}Zr	40.754	2.030×10^{-72}	2.241×10^{-51}	50.490	47.100	45.450
^{122}Ba		^{90}Zr	40.180	1.463×10^{-73}	1.592×10^{-52}	51.639	48.263	46.854
^{112}Ba	^{36}Ar	^{76}Sr	48.372	1.841×10^{-68}	2.411×10^{-47}	46.459	43.348	38.877
^{114}Ba		^{78}Sr	47.446	5.674×10^{-70}	7.290×10^{-49}	47.978	45.076	40.835
^{116}Ba		^{80}Sr	45.843	2.250×10^{-73}	2.794×10^{-52}	51.395	47.957	44.450
^{118}Ba		^{82}Sr	43.892	5.183×10^{-78}	6.161×10^{-57}	56.051	51.951	49.164
^{120}Ba		^{84}Sr	41.991	6.678×10^{-83}	7.595×10^{-62}	60.960	56.179	54.103
^{112}Ba	^{40}Ca	^{72}Kr	52.677	1.094×10^{-68}	1.561×10^{-47}	46.647	44.572	38.135
^{114}Ba		^{74}Kr	51.218	2.522×10^{-71}	3.499×10^{-50}	49.297	47.148	41.143
^{116}Ba		^{76}Kr	49.160	1.037×10^{-75}	1.380×10^{-54}	53.701	50.780	45.676
^{118}Ba		^{78}Kr	46.676	1.191×10^{-81}	1.506×10^{-60}	59.663	55.779	51.602
^{120}Ba		^{80}Kr	43.850	3.433×10^{-89}	4.077×10^{-68}	67.230	62.133	59.009

From tables 1 and 2, a comparison of ^{12}C decay from ^{112}Ba to that from the other heavier isotopes up to ^{122}Ba shows that the $\log_{10}(T_{1/2})$ value increases from 4.4548 s (for ^{112}Ba) to 39.2572 s (for ^{122}Ba). All the cases refer to doubly magic or nearly doubly magic daughter Sn nuclei. This will point to the fact that the exotic decay process slows down due to the presence of neutron excess in the parent nuclei.

The earlier studies done within CPPM clearly reveal that our model can very well reproduce the experimental half-lives of the nuclei. In addition, our model can be used to

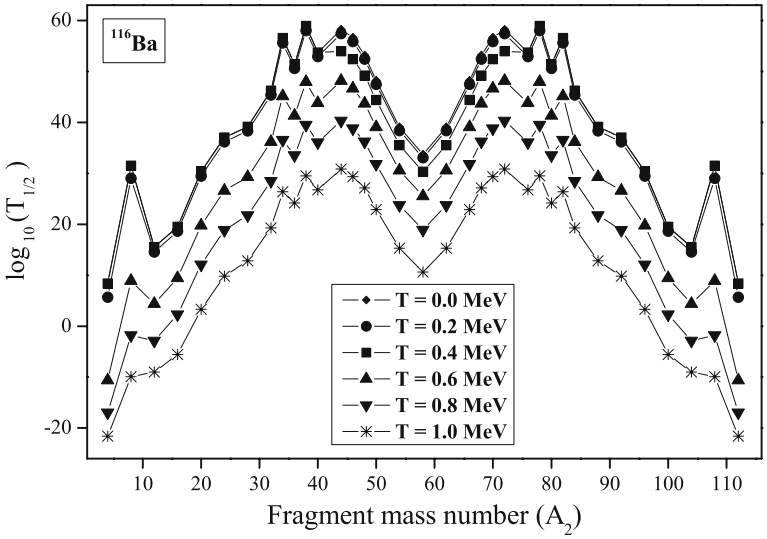

Figure 9. Variation of half-life with nuclear temperature for various clusters of ^{116}Ba.

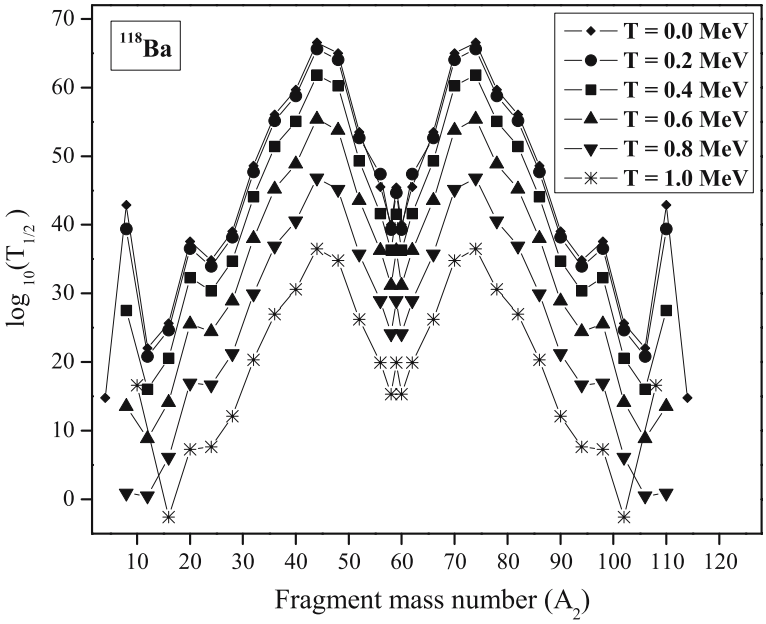

Figure 10. Variation of half-life with nuclear temperature for various clusters of ^{118}Ba.

evaluate the branching ratio of cluster decay with respect to α-decay. The branching ratio B of cluster decay with respect to α emission is given by

$$B = \frac{\lambda_{\text{cluster}}}{\lambda_{\text{alpha}}} = \frac{T_{1/2}^{\text{alpha}}}{T_{1/2}^{\text{cluster}}}. \tag{25}$$

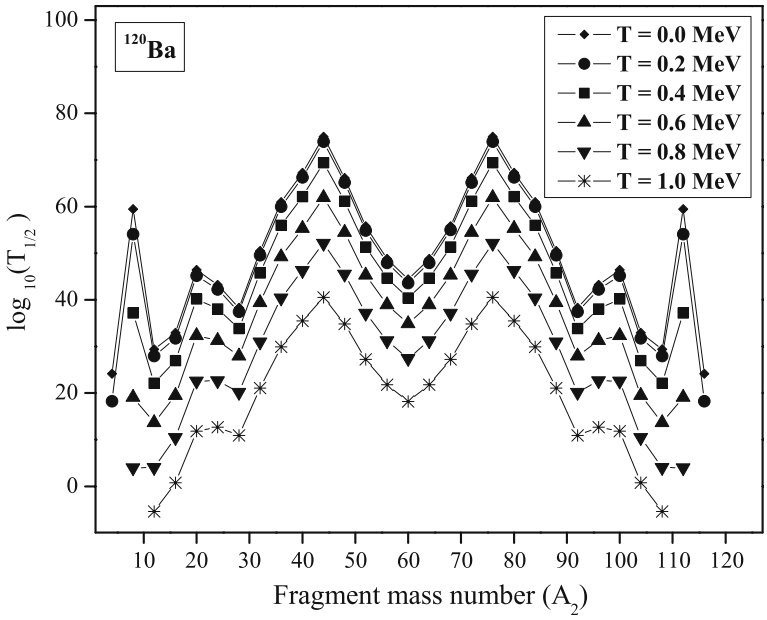

Figure 11. Variation of half-life with nuclear temperature for various clusters of ^{120}Ba.

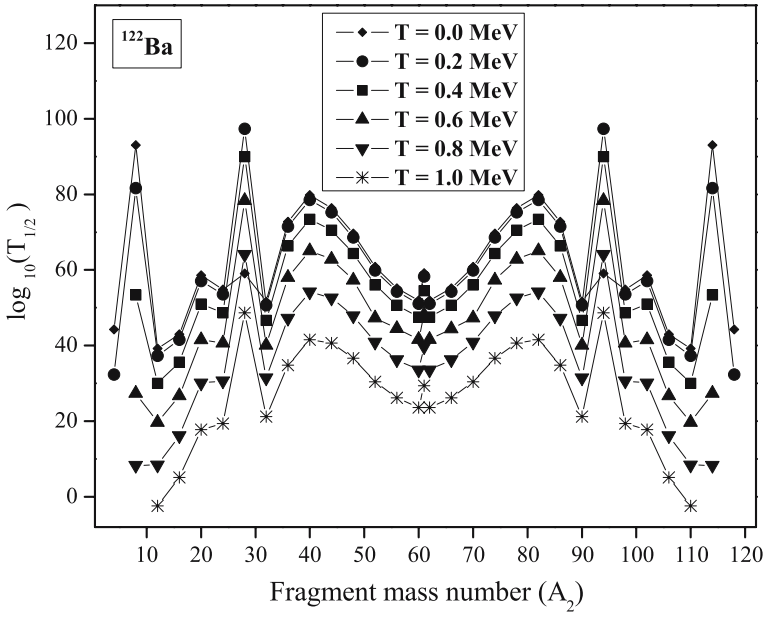

Figure 12. Variation of half-life with nuclear temperature for various clusters of ^{122}Ba.

In the present study, we have evaluated the branching ratio of ^{114}Ba for the emission of ^{12}C, using eq. (25) and is found to be 3.639×10^{-7}. The experimental upper limit [9] of branching ratio of ^{114}Ba was found to be $B < 3.400 \times 10^{-5}$. On comparing the computed branching ratio with the experimental value, it can be seen that the computed value exactly comes under this upper limit.

4. Conclusion

The half-life and other characteristics for the emission of various clusters from even–even isotopes of barium in the range $112 \leq A \leq 122$ have been studied using the Coulomb and proximity potential model. Most of the predicted values for ground-state decays are within the present experimental limit for the measurements ($T_{1/2} < 10^{30}$ s). The role of doubly magic daughter Sn nuclei in cluster decay process is evident from our study. A comparison of $\log_{10}(T_{1/2})$ value reveals that the exotic cluster decay process slows down due to the presence of neutron excess in the parent nuclei. Also comparison of half-lives for the ground and the excited systems shows that the probability of decay increases with rise in temperature, i.e., inclusion of excitation energy decreases $T_{1/2}$ values. The half-life values calculated using CPPM is found to be in good agreement with those values computed using UNIV and UDL.

References

[1] A Sandulescu, D N Poenaru and W Greiner, *Sov. J. Part. Nucl.* **11**, 528 (1980)
[2] H J Rose and G A Jones, *Nature* **307**, 245 (1984)
[3] A Sandulescu, Yu S Zamyatnin, I A Lebedev, V F Myasoedov, S P Tretyakova and D Hashegan, *J.I.N.R. Rapid Commun.* **5**, 84 (1984)
[4] R Bonetti and A Guglielmetti, *Rom. Rep. Phys.* **59**, 301 (2007)
[5] D N Poenaru, W Greiner and R Gherghescu, *Phys. Rev. C* **47**, 2030 (1993)
[6] S Kumar and R K Gupta, *Phys. Rev. C* **49**, 1922 (1994); *Phys. Rev. C* **51**, 17602 (1995); *J. Phys. G: Nucl. Part. Phys.* **22**, 215 (1996)
[7] Yu Ts Oganessian, Yu A Lazarev, V L Mikheev, Yu A Muzychka, I V Shirokovsky, S P Tretyakova and V K Utyonkov, *Z. Phys. A* **349**, 341 (1994)
[8] A Guglielmetti, R Bonetti, G Poli, P B Price, A J Westphal, Z Janas, H Keller, R Kirchner, O Klepper, A Piechaczek, E Roeckl, K Schmidt, A Plochocki, J Szerypo and B Blank, *Phys. Rev. C* **52**, 740 (1995)
[9] A Guglielmetti, R Bonetti, G Poli, R Collatz, Z Hu, R Kirchner, E Roeckl, N Gunn, P B Price, B A Weaver, A Westphal and J Szerypo, *Phys. Rev. C* **56**, R2912 (1997)
[10] C Mazzocchi, Z Janas, L Batist, V Belleguic, J Döring, M Gierlik, M Kapica, R Kirchner, G A Lalazissis, H Mahmud, E Roeckl, P Ring, K Schmidt, P J Woods and J Zylicz, *Phys. Lett. B* **532**, 29 (2002)
[11] G Audi, O Bersillon, J Blachot and A H Wapstra, *Nucl. Phys. A* **729**, 3 (2003)
[12] G Royer, R K Gupta and V Y Denisov, *Nucl. Phys. A* **632**, 275 (1998)
[13] S Landowne and C H Dasso, *Phys. Rev. C* **33**, 387 (1986)
[14] M Iriondo, D Jerrestan and R J Liotta, *Nucl. Phys. A* **454**, 252 (1986)
[15] R Blendowske, T Fliessbach and H Walliser, *Nucl. Phys. A* **464**, 75 (1987)
[16] S S Malik and R K Gupta, *Phys. Rev. C* **39**, 1992 (1989)
[17] S Kumar and R K Gupta, *Phys. Rev. C* **55**, 218 (1997)

[18] D Ni, Z Ren, T Dong and C Xu, *Phys. Rev. C* **78**, 044310 (2008)
[19] Z Ren, C Xu and Z Wang, *Phys. Rev. C* **70**, 034304 (2004)
[20] D Ni, Z Ren, K P Santhosh and B Priyanka, *Phys. Rev. C* **82**, 024311 (2010)
[21] R K Gupta, *Proceedings of the 5th International Conference on Nuclear Reaction Mechanisms* (1988, Verenna, Italy) edited by E Gadioli (Ricera Scientifica Educazione Permanente, Italy), in Pressel, P.416
S S Malik, S Singh, R K Puri, S Kumar and R K Gupta, *Pramana J. – Phys.* **32**, 419 (1989)
[22] R K Gupta, S Singh, R K Puri and W Scheid, *Phys. Rev. C* **47**, 561 (1993)
[23] S Kumar and R K Gupta, *Phys. Rev. C* **49**, 1922 (1994)
[24] S Kumar, D Bir and R K Gupta, *Phys. Rev. C* **51**, 1762 (1995)
[25] D N Poenaru, W Greiner and E Hourani, *Phys. Rev. C* **51**, 594 (1995)
[26] A Guglielmetti, B Blank, R Bonetti, Z Janas, H Keller, R Kirchner, O Klepper, A Piechaczek, A Plochocki, G Poli, P B Price, E Roeckl, K Schmidt, J Szerypo and A J Westphal, *Nucl. Phys. A* **583**, 867C (1995)
[27] Yu Ts Oganessian, Yu A Lazarev, V A Mikheev, Yu a Muzychka, I V Shirokovsky, S P Tretyakova and V K Utyonkov, *Z. Phys. A* **349**, 341 (1994)
[28] J Gomez del Campo, J L Charvet, A D'Onofrio, R L Auble, J R Beene, M L Halbert and H J Kim, *Phys. Rev. Lett.* **61**, 290 (1988)
[29] J Gomez del Campo, R L Auble, J R Beene, M L Halbert, H J Kim, A D'Onofrio and J L Charvet, *Phys. Rev. C* **43**, 2689 (1991)
[30] J Gomez del Campo *et al*, *Phys. Rev. C* **57**, R457 (1998)
[31] M La Commara *et al*, *Nucl. Phys. A* **669**, 43 (2000)
[32] A Sandulescu, Yu S Zamyatnin, I A Lebedev, V F Myasoedov, S P Tretyakova and D Hashegan, *J.I.N.R. Rapid Commun.* **5**, 84 (1984)
[33] K P Santhosh and A Joseph, *Proc. Int. Natl. Symp. Nucl. Phys. (India) B* **43**, 296 (2000)
[34] K P Santhosh and A Joseph, *Pramana – J. Phys.* **58**, 611 (2002)
[35] K P Santhosh and A Joseph, *Pramana – J. Phys.* **62**, 957 (2004)
[36] K P Santhosh and A Joseph, *Pramana – J. Phys.* **64**, 39 (2005)
[37] K P Santhosh, B Priyanka and M S Unnikrishnan, *Nucl. Phys. A* **889**, 29 (2012)
[38] K P Santhosh and B Priyanka, *Eur. Phys. J. A* **49**, 66 (2013)
[39] K P Santhosh and B Priyanka, *Nucl. Phys. A* **929**, 20 (2014)
[40] K P Santhosh and B Priyanka, *Int. J. Mod. Phys. E* **23**, 1450059 (2014)
[41] K P Santhosh, Indu Sukumaran and B Priyanka, *Nucl. Phys. A* **935**, 28 (2015)
[42] K P Santhosh and B Priyanka, *Phys. Rev. C* **89**, 064604 (2014)
[43] K P Santhosh and B Priyanka, *Phys. Rev. C* **90**, 054614 (2014)
[44] K P Santhosh and V Bobby Jose, *Nucl. Phys. A* **922**, 191 (2014)
[45] D N Poenaru, R A Gherghescu and W Greiner, *Phys. Rev. C* **83**, 014601 (2011)
[46] C Qi, F R Xu, R J Liotta, R Wyss, M Y Zhang, C Asawatangtrakuldee and D Hu, *Phys. Rev. C* **80**, 044326 (2009)
[47] Y J Shi and W J Swiatecki, *Nucl. Phys. A* **438**, 450 (1985)
[48] Y J Shi and W J Swiatecki, *Nucl. Phys. A* **464**, 205 (1987)
[49] J Blocki, J Randrup, W J Swiatecki and C F Tsang, *Ann. Phys (NY)* **105**, 427 (1977)
[50] J Blocki and W J Swiatecki, *Ann. Phys. NY* **132**, 53 (1981)
[51] D N Poenaru, M Ivascu, A Sandulescu and W Greiner, *Phys. Rev. C* **32**, 572 (1985)
[52] M Wang, G Audi, A H Wapstra, F G Kondev, M MacCormick, X Xu and B Pfeiffer, *Chin. Phys. C* **36**, 1603 (2012)
[53] H Koura, T Tachibana, M Uno and M Yamada, *Prog. Theor. Phys.* **113**, 305 (2005)
[54] D N Poenaru and W Greiner, *J. Phys. G.: Nucl. Part. Phys.* **17**, S443 (1991)
[55] D N Poenaru and W Greiner, *Phys. Scr.* **44**, 427 (1991)
[56] D N Poenaru, I H Plonski and W Greiner, *Phys. Rev. C* **74**, 014312 (2006)

[57] D N Poenaru, I H Plonski, R A Gherghescu and W Greiner, *J. Phys. G.: Nucl. Part. Phys.* **32**, 1223 (2006)
[58] R Blendowske and H Walliser, *Phys. Rev. Lett.* **61**, 1930 (1988)
[59] R Blendowske, T Fliessbach and H Walliser, *Nuclear decay modes* (Institute of Physics Publishing, Bristol, 1996) Chap. 7, p. 337
[60] M Iriondo, D Jerrestam and R J Liotta, *Nucl. Phys. A* **454**, 252 (1986)
[61] C Qi, F R Xu, R J Liotta and R Wyss, *Phys. Rev. Lett.* **103**, 072501 (2009)